18. Computational Approach to the Receptor-Bound Conformation of Cyclosporin A

Matthias Köck[1]), **Gerhard Müller**[2]), and **Horst Kessler***

Organisch-chemisches Institut, Technische Universität München, Lichtenbergstr. 4, D–85747 Garching

(30.VII.93)

The conversion of the conformation of cyclosporin A (CsA) observed in $CHCl_3$ to the receptor-bound state is investigated by two molecular-mechanics methods, template forcing and dynamic forcing. The conformations of CsA in $CHCl_3$ and complexed with LiCl in THF as determined by NMR are used as starting structures. The transition starting from the CsA/$CHCl_3$-derived conformation is hindered by steric interactions of two side chains (MeBmt[1] and Val[5]). While starting with the CsA/LiCl-derived conformation, the conversion is facile. It is illustrated that these calculations, which are of artificial character, using only the starting and final structures of the observed conformational transition during the receptor-binding event, allow an insight into the interactions between the substrates and receptor in terms of an induced fit.

Introduction. – Cyclosporin A, cyclo(-MeBmt[1]-Abu[2]-Sar[3]-MeLeu[4]-Val[5]-MeLeu[6]-Ala[7]-D-Ala[8]-MeLeu[9]-MeLeu[10]-MeVal[11]-), is an immunosuppressive drug widely used clinically to prevent graft rejection in organ transplantations [1]. It suppresses the cellular and humoral immune response through inhibition of the expression of interleukin-2 from T-cells or of interleukin-1 from B-cells. The major cytosolic receptor of CsA is cyclophilin (CyP) [2], a peptidyl-prolyl-*cis/trans*-isomerase (PPIase) [3]. It was shown recently that the complexation of CsA with CyP is only the first step of a multiple-step transduction through the cytosol. The CsA-CyP complex interacts with calcineurin A and inhibits its phosphatase activity, whereas no inhibitory effect was found for CsA or CyP alone [4]. Therefore, the complexation of CsA with CyP is necessary for immunosuppressive activity. The role of the inhibition of the PPIase activity or to protein folding of CyP by CsA with regard to the immunosuppressive activity is still not clear [4].

Background. – The structures of CsA in the crystal [5] and in $CDCl_3$ [6], of CyP [7], of the receptor-bound structure of CsA [8], and of the complex of CsA with CyP [9] both by X-ray and NMR spectroscopy were determined. CsA undergoes a drastic conformational rearrangement when changing from the structure in organic solution to the receptor-bound state. The conformation of CsA determined by NMR in $CDCl_3$ and in the crystal shows an antiparallel β-pleated sheet stabilized by three intramolecular H-bonds involving a βII′-turn with Sar[3] and MeLeu[4] in the central $i + 1$ and $i + 2$ positions (see *Fig. 1*). The β-hairpin includes residues 11–7, whereas the amino acids 7–11 form a loop with a *cis*-peptide bond between residues 9 and 10. A closer inspection of this loop reveals a

[1]) Present address: Institut für Organische Chemie, Universität Frankfurt, Marie-Curie-Str. 11, D–60439 Frankfurt am Main.

[2]) Present address: *Glaxo S.p.A.*, Research Centre – Medicinal Chemistry, Computer-Aided Drug Design, Via A. Fleming 4, I–37100 Verona.

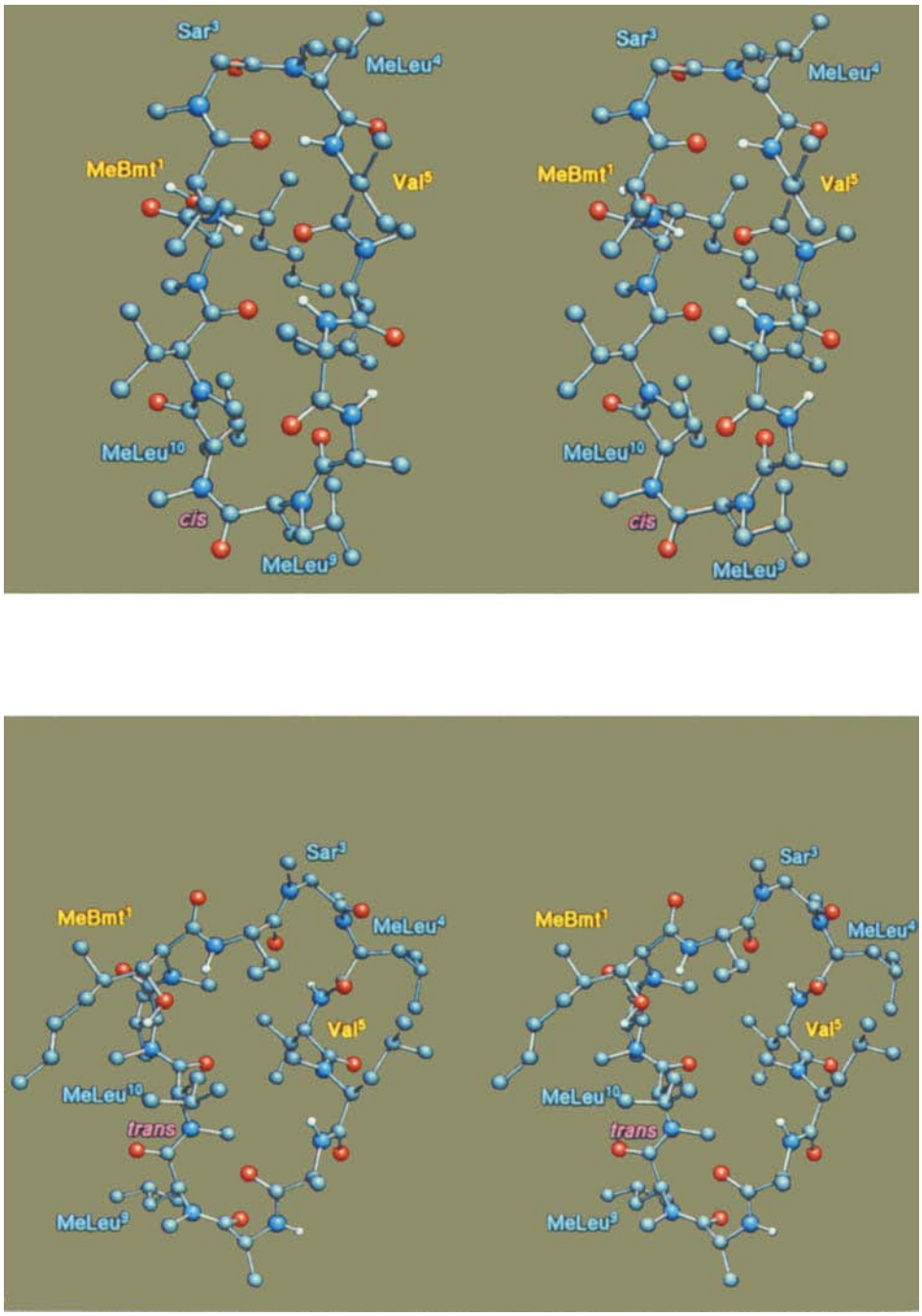

Fig. 1. *Stereoplots of the NMR-derived conformations of CsA in* $CDCl_3$ (top), *CsA/LiCl in THF* (bottom), *and the receptor-bound structure* (right)

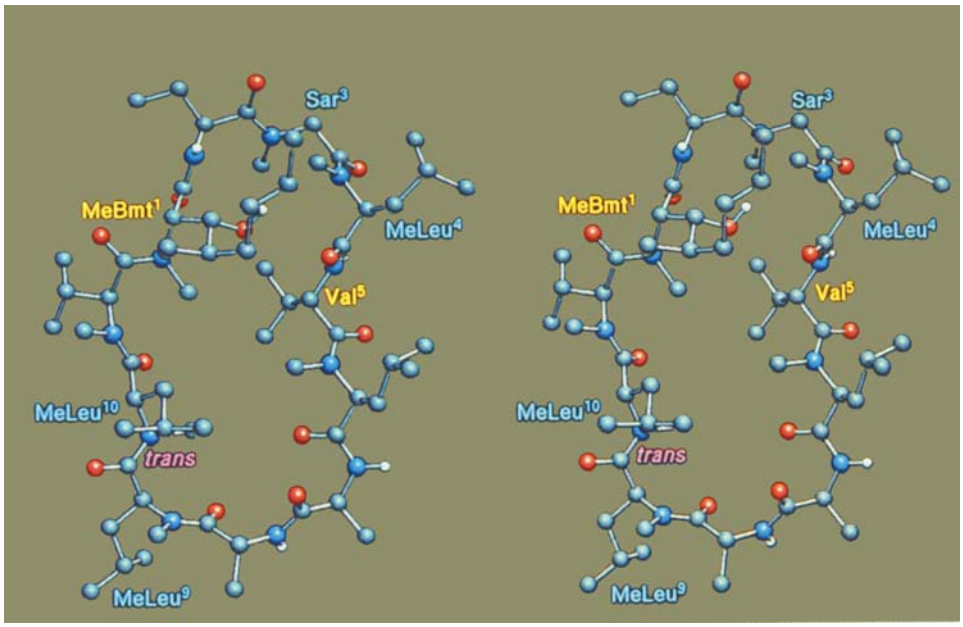

βVIb-turn conformation at this position [10]. In contrast, the conformation of CsA complexed with LiCl in THF has an expanded backbone structure with no transannular H-bonds (see *Fig. 1*) [11]. This substantial structural change is induced by the interaction of peptide functionalities with Li cations. The configuration of the peptide bond between MeLeu^9 and MeLeu^{10} is *trans*. Additionally, a type-II′ β-turn-like conformation is found for residues 8 and 9. The receptor-bound structure of CsA is completely different to those found in solution or in the crystal. No secondary structural elements are formed, and the 9,10-peptide bond is in *trans* configuration, as found for the CsA/LiCl system (see *Fig. 1*). The residues 9–3 are directed towards the binding domain of CyP, while the remainder is exposed to the solvent. *Rich* and coworkers showed that the *cis*-MeLeu^9-MeLeu^{10} CsA isomer is completely inactive as a PPIase inhibitor on a few-min time scale, whereas the *trans* isomer (CsA/LiCl in THF) is a tight-binding PPIase inhibitor [12]. For a detailed comparison of these three conformations, a list of the backbone dihedrals is given in the *Table*.

The aim of this investigation is to simulate transition pathways, starting with the above mentioned different conformations of CsA, as determined by NMR in $CHCl_3$ and complexed with LiCl in THF, to the receptor-bound structure using two different molecular-mechanics methods. The *template-forcing method* employs energy minimization to induce an optimized fit of the NMR-derived starting conformations to the receptor-bound template structure. Alternatively, the *dynamic-forcing method* utilizes molecular-dynamics (MD) simulations and, therefore, takes kinetic-energy contributions into account, which is necessary to overcome barriers on the molecular hypersurface for the course from the starting to the target conformation. By these computational approaches, we intented to simulate an induced fit of the substrates by exerting intrinsic conforma-

Table. *Comparison of the Backbone Dihedral Angles of Three Different Conformations of CsA, Determined by NMR in $CDCl_3$* [6], *in LiCl/THF* [11], *and in the Receptor-Bound State* [8]

Residue	Dihedral	Angle [°]		
		$CsA/CHCl_3$	CsA/LiCl	CsA-CyP
	ϕ	–89	–153	–92
MeBmt[1]	ψ	112	–79	–178
	ω	169	167	180
	ϕ	–97	168	–116
Abu[2]	ψ	100	–50	79
	ω	176	180	180
	ϕ	79	–63	139
Sar[3]	ψ	–108	130	–66
	ω	162	–153	180
	ϕ	–122	59	–112
MeLeu[4]	ψ	30	95	93
	ω	174	169	180
	ϕ	–104	–38	–92
Val[5]	ψ	123	113	134
	ω	167	–176	180
	ϕ	–82	–113	–122
MeLeu[6]	ψ	88	–85	173
	ω	178	–169	180
	ϕ	–67	–96	–45
Ala[7]	ψ	54	128	162
	ω	180	171	180
	ϕ	80	76	108
D-Ala[8]	ψ	–137	–118	–165
	ω	–177	163	180
	ϕ	–125	–119	–122
MeLeu[9]	ψ	116	87	74
	ω	–3	177	180
	ϕ	–131	–110	–117
MeLeu[10]	ψ	86	128	171
	ω	173	–157	180
	ϕ	–120	–111	–126
MeVal[11]	ψ	133	70	67
	ω	154	180	180

tional restraints, realized by penalty terms within the applied force field. Both methods should provide a more detailed insight into the large conformational changes of the substrates during receptor binding.

Methods. – All calculations were carried out on *Silicon-Graphics-4D/240SX* and *-4D/70GTB* computers using the Discover program [13]. The treatment of an explicit solvent environment, especially in the dynamic-forcing simulations, was computational prohibitive, therefore, the calculations were carried out *in vacuo*. However, in a systematic investigation of different CsA derivatives, it turned out that calculations *in vacuo* and in a solvent box ($CHCl_3$) lead to almost the same results due to the strong hydrophobic character of CsA [14]. To diminish long-range effects due to overemphasized coulombic forces and to mimic the dielectric properties of an aqueous environment, a dielectric permittivity of 80 was used.

The template-forcing method [15] is based on energy-minimization techniques to optimize the adaptation of a starting structure to a target conformation (template). The standard CVFF force-field (*Eqn. 1*) is used with an additional penalty term (*Eqn. 2*), that describes the root mean square (r.m.s.) deviation between the coordinates of both structures. The dynamic-forcing method [16] employs dihedral restraining incorporated in molecular dynamics. Comparable to distance restraining, this is accomplished by definition of an appropriate target function within the potential-energy function (CVFF; *Eqn. 3*).

$$V_{\mathrm{CVFF}}(r) = \sum_{bonds} \frac{1}{2} k_b (b - b_0)^2 + \sum_{angles} \frac{1}{2} k_\Theta (\Theta - \Theta_0)^2 + \sum_{\substack{out\text{-}of\text{-} \\ planes}} \frac{1}{2} k_\xi (\xi - \xi_0)^2 + \tag{1}$$

$$+ \sum_{dihedrals} k_\phi (1 + \cos(n\phi - \delta)) + \Sigma\Sigma_{i<j} \left(\frac{C_{12}}{r_{ij}^{12}} - \frac{C_6}{r_{ij}^6} + \frac{q_i q_j}{4\pi\varepsilon_0 \varepsilon_r r_{ij}} \right)$$

$$V_{\mathrm{tf}} = V_{\mathrm{CVFF}} + \Sigma k_{\mathrm{tf}} (r - r_0)^2, \qquad r_0 = \text{template coordinates} \tag{2}$$

$$V_{\mathrm{df}} = V_{\mathrm{CVFF}} + \Sigma k_{\mathrm{df}} (\psi - \psi_0)^2, \quad \psi_0 = \text{target dihedrals} \tag{3}$$

Especially monitoring the trajectories of the dynamic-forcing simulations allows one to detect and to characterize reasonable conformational pathways between the two corresponding boundary structures.

Results and Discussion. – For all template-forcing approaches, we chose 10000 steps of EM with a whole series of force constants (k_{tf}). With $k_{\mathrm{tf}} \geq 175$ kcal·mol^{-1}·Å^{-2}, the transition from the conformation of CsA in $CHCl_3$ to the CyP-bound structure was obtained (see *Fig. 2*). With a smaller k_{tf}, the conformational transition was not observed,

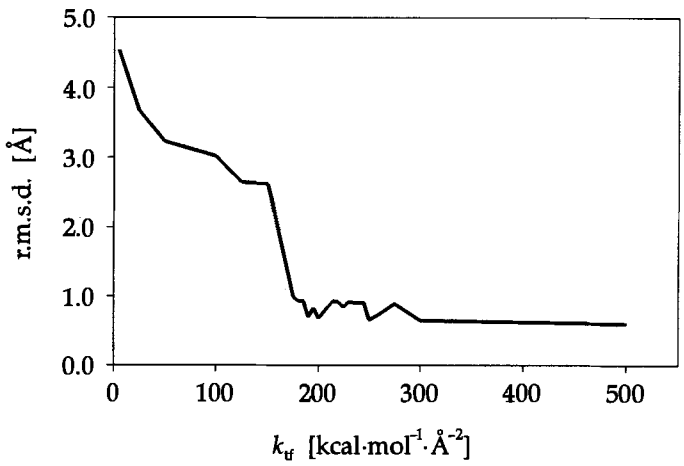

Fig. 2. *Analysis of the template-forcing simulations of the CsA/CHCl$_3$ system.* The achieved r.m.s. deviations for superimposing the conformation after the forcing onto the target are shown against the force constant of the penalty potential. With $k_{\mathrm{tf}} \geq 175$ kcal·mol^{-1}·Å^{-2}, the desired transition to the receptor-bound conformation is achieved.

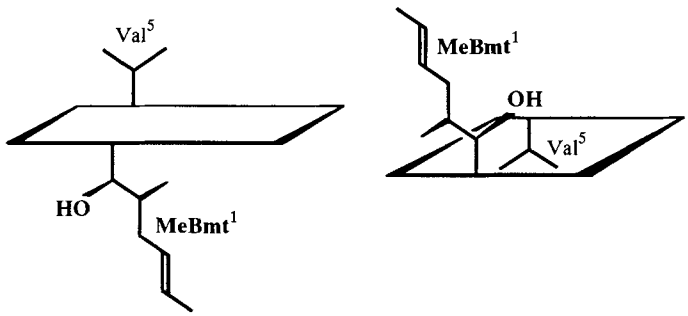

Fig. 3. *Schematic representation of the arrangement of the MeBmt*^{1} *and Val*^{5} *side chains in CsA in* $CDCl_3$ (left) *and the receptor-bound state* (right)

hindered by collision of the side chains of MeBmt^1 and Val^5 (see *Fig. 3*). This steric conflict cannot be resolved with smaller k_{tf} due to the applied minimization technique, which is *per definitionem* unable to overcome conformational-energy barriers. For the CsA/LiCl system, the desired transition was achieved with a k_{tf} of only 60 kcal·mol^{-1}·Å^{-2}. The adaptation of the target structure for the CsA/LiCl system at much lower forcing potentials is in accordance with the closer conformational relation of both, the starting and the target structure, when compared to the CsA conformation observed in $CHCl_3$. In this regard, the *cis* to *trans* conversion between residues 9 and 10 may be the most important difference.

For the dynamic-forcing simulations it was impossible to reach a satisfactory structural complementarity with the receptor-bound structure using all dihedral angles (backbone and side chains) at once. Even increasing the temperature to 1000 K to raise the kinetic-energy contribution was not successful. Therefore, different simulation protocols were tested to achieve the transition: First, a simulation covering 100 ps with a forcing potential for only the dihedral angles of the receptor-binding sequence (amino acids 9–3 of CsA) was performed; second, identical dihedrals were used as before, but the conformational forcing was introduced in three steps, starting with residues 11 and 1 (40 ps), extension of the forced region to residues 10, 11, 1, and 2 (40 ps), followed by a further 40 ps MD simulation including the amino acids 9–3; third, the introduction of the conformational forcing was divided into six steps (20 ps, residue 9; 20 ps, residues 9 and 10; 20 ps, residues 9–11; 20 ps, residues 9–11 and 1; 20 ps, residues 9–11, 1 and 2; 20 ps, residues 9–11 and 1–3). All these calculations were run at 300 K with several different force constants (k_{df}), but again without any success. It turned out that the main problem of the simulation is the crossing of the side chains of MeBmt^1 and Val^5 (see *Fig. 3*). These two side chains have to change their spatial exposition relative to the peptide-ring plane during the conformational change from the $CHCl_3$-derived structure to the receptor-bound conformation.

For this reason, we started another approach that centered the forcing restraints on these two residues, followed by a stepwise introduction of the flanking amino acids in three subsequent steps: *a*) residues 1 and 5; *b*) residues 11, 1, 2 and 4, 5–6; *c*) residues 10, 11, 1–7; *d*) all residues (see *Fig. 4*). For every step, a simulation of 30 ps was performed with different k_{df} for ϕ and ψ, whereas for ω, k_{df} was always 100 kcal·mol^{-1}·rad^{-2}. For

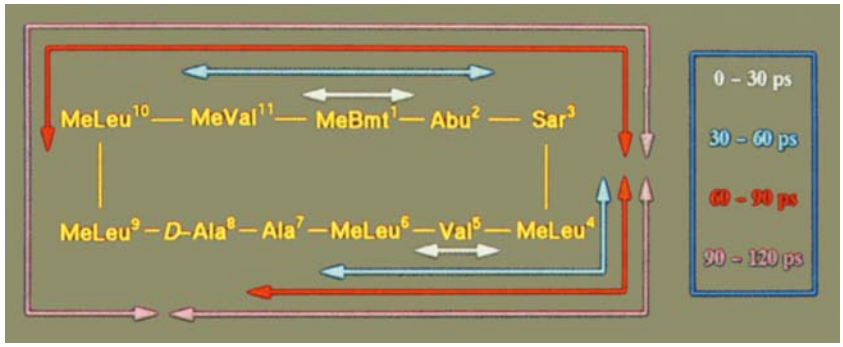

Fig. 4. *Schematic representation of the successfully applied protocol of the dynamic-forcing simulation for the transition of CsA conformation in $CDCl_3$ to the receptor-bound structure.* The different coloured arrows refer to the simulation periods given on the right.

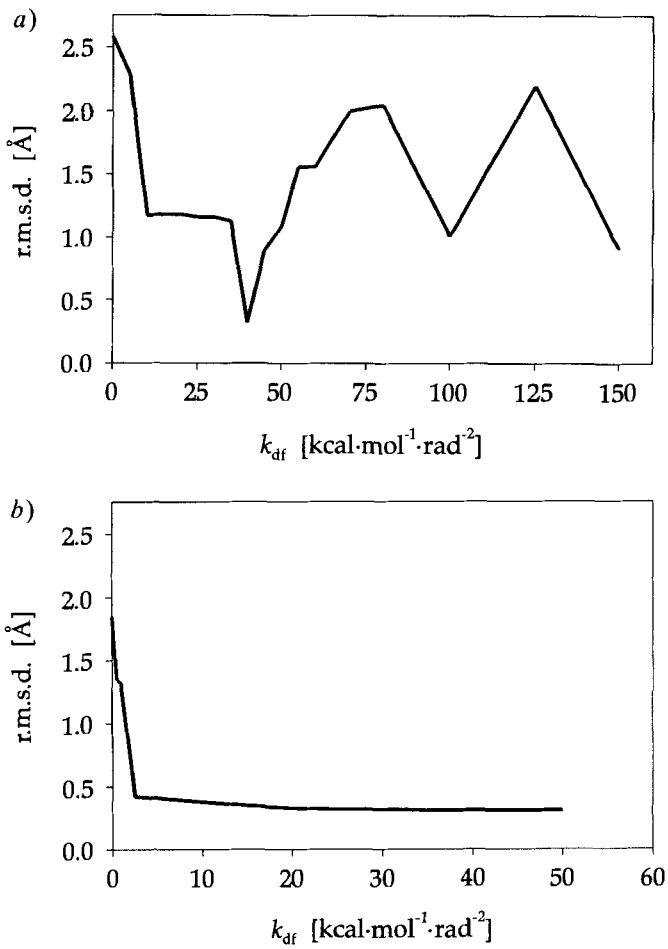

Fig. 5. *Analysis of the dynamic-forcing simulations of* a) *CsA and* b) *CsA/LiCl.* The r.m.s. deviation for the superposition of the simulation results to the receptor-bound structure are shown against the force constant of the penalty potential refering to the backbone atoms. *Fig. 5a* clearly proves that the desired conformational transition is achieved only with k_{df} = 40 kcal·mol^{-1}·rad^{-2}, while all other dynamic-forcing simulations result in structures with a backbone r.m.s. deviation greater than 1.0 Å. *Fig. 5b* indicates the close structural relationship between the CsA/LiCl conformation and the receptor-bound state, since the target structure is adopted at low forcing potentials.

$k_{df} = 40$ kcal·mol^{-1}·rad^{-2}, a satisfactory adaptation to the receptor-bound structure was found for the CsA/$CDCl_3$ conformation (r.m.s. deviation for superposition of all atoms, 0.70 Å, for the backbone, 0.32 Å). For larger or smaller k_{df}, transitions to the target structure were not observed. It is interesting to note that increasing of the forcing potential did not result in increased structural complementarity (see *Fig. 5a*). Instead, an energetic window of the artificial forcing achieving the desired transition was detected. Similar results were obtained from simulations of different derivatives of CsA (data not shown) [17].

Application of higher restraining force constants traps the molecule obviously in metastable minima. To satisfy the complete set of restraints would require an intermediate violation of few dihedral restraints that adopt already their target values. With increasing forcing potential, this becomes more unlikely, and the transition to the target conformation is prevented by these artificially generated high energetic barriers.

A possible transition pathway monitored by the dynamics simulation is depicted by five snapshots in *Fig. 6*. In the course of the simulation, the two residues MeBmt^1 and Val^5 that prevented the transition in the template-forcing calculations, alter their side-chain orientations by different mechanisms. While the Val^5 isopropyl group passes through the peptide ring, the more bulky MeBmt^1 side chain shifts through the outer surface. The isomerism of the 9,10-peptide bond from *cis*- to *trans*-configuration occurs during the last of the four simulation periods (see last paragraph), when the forcing potential is applied to the involved residues.

The same procedure was applied to the structure of CsA/LiCl in THF [11]. For this system, only a very small k_{df} is necessary to reach the receptor-bound structure (*Fig. 5b*) under the simulation conditions developed for the CsA/$CHCl_3$ system. The conformational analysis of CsA/LiCl in THF resulted in a structure [11], which is closely related to the receptor-bound conformation, confirmed by a r.m.s. deviation of 1.85 Å for the superposition of all backbone atoms. The corresponding r.m.s. deviation for superposition of the CsA/$CHCl_3$ and CsA-CyP pair of 2.68 Å indicates the structural diversity of these two conformations. In the NMR-derived structure, the peptide bond between the residues 9 and 10 is already in *trans*-configuration as in the receptor-bound state. The orientation of the side chains of MeBmt^1 and Val^5 with regard to the peptide-ring plane is also in accordance with the receptor-bound structure of CsA.

The results obtained here for both systems are in accordance with the kinetic data of the inhibition of the PPIase activity of CyP with CsA/LiCl, which shows a faster inhibitory kinetic of the PPIase activity of CyP compared to CsA in THF. This indicates substantially different accessible transition pathways for both systems and that the CsA/LiCl system demonstrates a closer conformational relation to the target state. The template-forcing simulations as well as the dynamic-forcing calculations allowed the identification of two residues, MeBmt^1 and Val^5, critical for the binding event to CyP. Their dynamic reorientation, together with the 9,10 *cis*/*trans*-isomerism, play a substantial role for achieving receptor complementary structures.

From a methodological point of view, it seems rather unexpected that molecular-dynamics simulations did not allow an easy transition of the chloroform-derived conformation to the target structure. Since molecular-dynamics techniques allow to overcome energetic barriers due to interconversion of kinetic- and potential-energy contributions, one would have expected a more rapid and facile structural transition.

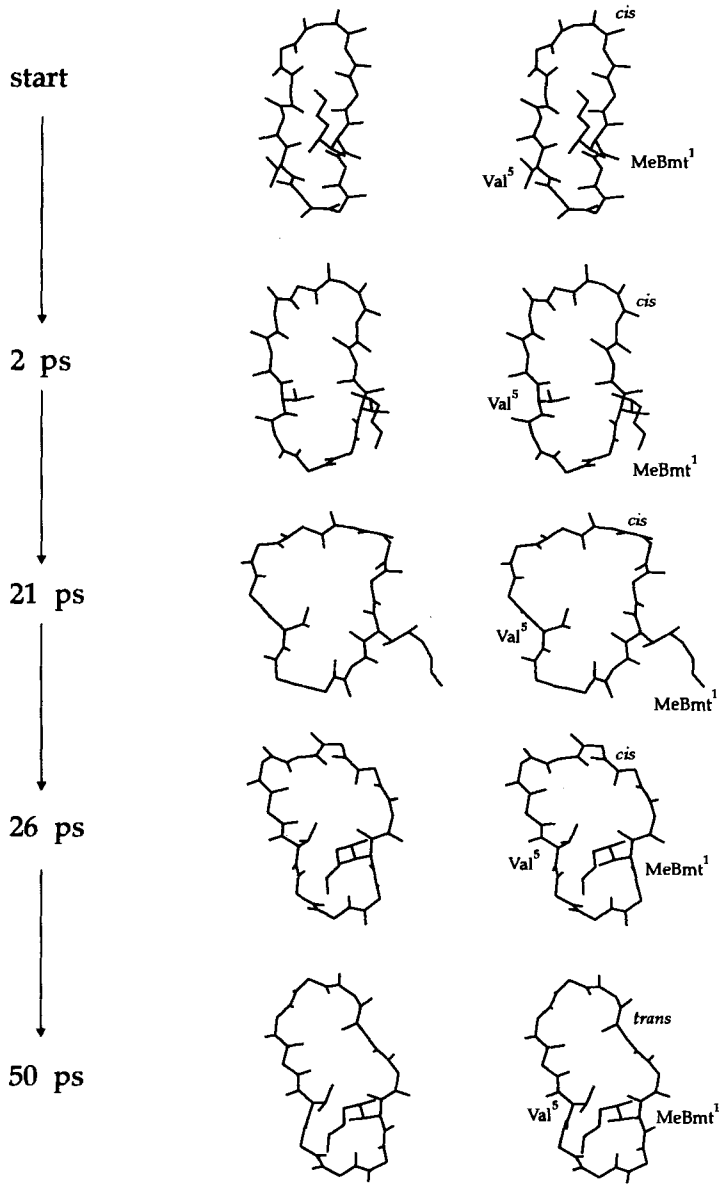

Fig. 6. *Stereoplot of selected intermediates taken from the dynamic-forcing trajectory of CsA.* A transition to the receptor-bound conformation is performed by a twist of the Val^5 side chain inward through the ring, while the side chain of $MeBmt^1$ changes its relative exposition by a shift to the outside of the peptide ring. The isomerism of the 9,10-peptide bond occurs during the last of the four simulation periods (see text).

Conclusion. – In the investigations, the conformational transition of CsA ($CDCl_3$) to the receptor-bound structure was examined with computational techniques. As the three-dimensional structure of the receptor binding site is not publically available, this approach mimics the driving force on the substrate to adopt the complementary conformation of the receptor binding site. The template-forcing technique, based on minimization strategies, resulted in conformations that obviously remained in metastable minima on the artificially distorted energy surface. Including contributions of kinetic energy, as in dynamic-forcing simulations, enabled the systems to overcome conformational barriers. A general statement about the path of the conformational transition is not possible with the applied protocol, because a biased procedure was applied. However, it is interesting to note that the calculations show a distinct channel for the conformational transition. Taking all simulation results together, it was by no means an easy task to induce the receptor-bound conformation by exploiting 'molecule-inherent' forces, *i.e.* artificial dihedral restraints. One could conclude that the receptor environment has to provide the necessary energy contributions during the initial stage of the binding event, to compensate some high-energy transitions of the substrate conformation in the course of binding.

As long as three-dimensional structures of receptor binding sites are not commonly available, the outlined approaches will serve as powerful computational tools in order to identify critical substrate residues for the binding event, provided the solution conformation as well as the receptor-bound structure of the substrate are solved with atomic resolution. If the conformational reorientation of such residues is identified as a rate-limiting step for achieving receptor complementarity, the presented procedures may help to develop new ideas for substrate design in a more dynamic fashion; a new access to an indirect drug design becomes feasible.

Financial support from the *Deutsche Forschungsgemeinschaft* and *Fonds der Chemischen Industrie* is gratefully acknowledged. *G.M.* and *M.K.* thank the *Fonds der Chemischen Industrie* for fellowships. Discussions with Prof. *D. Rich* are greatly acknowledged. We also thank Dr. *Dale F. Mierke* for his critical reading of this manuscript and Prof. *K. Wüthrich*, Zürich, Switzerland, as well as Dr. *S. W. Fesik*, Illinois, U.S.A., for the atomic coordinates of their structures of CsA bound to cyclophilin.

REFERENCES

[1] A. Rüegger, M. Kuhn, H. Lichti, H.-R. Loosli, R. Huguenin, C. Quiquerez, A. von Wartburg, *Helv. Chim. Acta* **1976,** *59,* 1075; M. Dreyfuss, E. Härri, H. Hofmann, H. Kobel, W. Pache, H. Tscherter, *Eur. J. Appl. Microbiol.* **1976,** *3,* 125; J. F. Borel, C. Feurer, H. U. Gubler, H. Stähelin, *Agents Actions* **1976,** *6,* 468.

[2] R. E. Handschuhmacher, M. W. Harding, J. Rice, R. J. Drugge, D. W. Speicher, *Science* **1984,** *226,* 544; M. W. Harding, R. E. Handschuhmacher, D. W. Speicher, *J. Biol. Chem.* **1986,** *261,* 8547.

[3] N. Takahashi, T. Hayano, M. Suzuki, *Nature (London)* **1989,** *337,* 473; G. Fischer, B. Wittmann-Liebold, K. Lang, T. Kiefhaber, F. X. Schmid, *ibid.* **1989,** *337,* 476.

[4] J. Friedman, I. Weissman, *Cell* **1991,** *66,* 799; J. Liu, J. D. Farmer, Jr., W. S. Lane, J. Friedman, I. Weissman, S. L. Schreiber, *ibid.* **1991,** *66,* 807; M. K. Rosen, S. L. Schreiber, *Angew. Chem.* **1992,** *104,* 413; *ibid. Int. Ed.* **1992,** *31,* 384.

[5] H.-R. Loosli, H. Kessler, H. Oschkinat, H.-P. Weber, T. J. Petcher, A. Widmer, *Helv. Chim. Acta* **1985,** *68,* 682.

[6] H. Kessler, M. Köck, T. Wein, M. Gehrke, *Helv. Chim. Acta* **1990,** *73,* 1818.

[7] J. Kallen, C. Spitzfaden, M. G. M. Zurini, G. Wider, H. Widmer, K. Wüthrich, M. D. Walkinshaw, *Nature (London)* **1991,** *353,* 276; K. Wüthrich, C. Spitzfaden, K. Memmert, H. Widmer, G. Wider, *FEBS Lett.* **1991,** *285,* 237; K. Wüthrich, B. von Freyberg, C. Weber, G. Wider, R. Traber, H. Widmer, W. Braun, *Science* **1991,** *254,* 953.

[8] S.W. Fesik, R.T. Gampe, Jr., T.F. Holzman, D.A. Egan, R. Edalji, J.R. Luly, R. Simmer, R. Helfrich, V. Kishore, D.H. Rich, *Science* **1990,** *250,* 1406; C. Weber, B. Wider, B. von Freyberg, R. Traber, W. Braun, H. Widmer, K. Wüthrich, *Biochemistry* **1991,** *30,* 6563; S.W. Fesik, R.T. Gampe, Jr., H.L. Eaton, G. Gemmecker, E.T. Olejniczak, P. Neri, T.F. Holzman, D.A. Egan, R. Edalji, R. Simmer, R. Helfrich, J. Hochlowski, M. Jackson, *ibid.* **1991,** *30,* 6574.

[9] S.W. Fesik, P. Neri, R. Meadows, E.T. Olejniczak, G. Gemmecker, *J. Am. Chem. Soc.* **1992,** *114,* 3165; C. Spitzfaden, H.-P. Weber, W. Braun, J. Kallen, G. Wider, H. Widmer, M.D. Walkinshaw, K. Wüthrich, *FEBS Lett.* **1992,** *300,* 291.

[10] G. Müller, M. Gurrath, M. Kurz, H. Kessler, *Proteins: Struct. Funct. Genet.* **1993,** *15,* 235.

[11] M. Köck, H. Kessler, D. Seebach, A. Thaler, *J. Am. Chem. Soc.* **1992,** *114,* 2676.

[12] J.L. Kofron, P. Kuzmic, V. Kishore, G. Gemmecker, S.W. Fesik, D. Rich, *J. Am. Chem. Soc.* **1992,** *114,* 2670.

[13] 'DISCOVER' and 'INSIGHT II', commercially available from *Biosym Technologies Inc.,* 10065 Barnes Canyon Rd, San Diego, CA 92121.

[14] M. Köck, Dissertation, Technische Universität München, 1992.

[15] R.S. Struthers, J. Rivier, A.T. Hagler, in 'Conformationally Directed Drug Design: Peptides and Nucleic Acids as Templates or Targets', Eds. J.A. Vida and M. Gordon, American Chemical Society, Washington, DC, 1984, p. 239.

[16] R.S. Struthers, G. Tanaka, S.C. Koerber, T. Solmajer, E.L. Baniak, L.M. Gierasch, W. Vale, J. Rivier, A.T. Hagler, *Proteins: Struct. Funct. Genet.* **1990,** *8,* 295.

[17] M. Köck, G. Müller, H. Kessler, 'Dynamic Forcing zur Formulierung von Struktur-Wirkungsbeziehungen verschiedener Cyclosporin-Derivate', poster presentation in the '6. Workshop Molecular Modeling', 26.5.–27.5.92, Darmstadt, Germany; M. Köck, G. Müller, H. Kessler, in 'Peptides 1992, Proc. 22nd Eur. Pept. Symp.', Eds. C.H. Schneider and A.N. Eberle, ESCOM, Leiden, 1993, p. 511.